Energy relaxation at quantum Hall edge

Levkivskyi, Ivan; Sukhorukov, Eugene

How to cite

LEVKIVSKYI, Ivan, SUKHORUKOV, Eugene. Energy relaxation at quantum Hall edge. In: Physical review. B, Condensed matter and materials physics, 2012, vol. 85, n° 7. doi: 10.1103/PhysRevB.85.075309

This publication URL: https://archive-ouverte.unige.ch/unige:36325
Publication DOI: 10.1103/PhysRevB.85.075309

Energy relaxation at quantum Hall edge

Ivan P. Levkivskyi and Eugene V. Sukhorukov
Département de Physique Théorique, Université de Genève, CH-1211 Genève 4, Switzerland
(Received 15 November 2011; published 10 February 2012)

In this work, we address the recent experiments [C. Altimiras *et al.*, Nat. Phys. **6**, 34 (2010); H. le Sueur *et al.*, Phys. Rev. Lett. **105**, 056803 (2010); C. Altimiras *et al.*, Phys. Rev. Lett. **105**, 226804 (2010)], where an electron distribution function at the quantum Hall (QH) edge at filling factor $\nu = 2$ has been measured with high precision. It has been reported that the energy of electrons injected into one of the two chiral edge channels with the help of a quantum point contact (QPC) is equally distributed between them, in agreement with earlier predictions, one being based on the Fermi gas approach [A. M. Lunde *et al.*, Phys. Rev. B **81**, 041311(R) (2010)] and the other utilizing the Luttinger-liquid theory [P. Degiovanni *et al.*, Phys. Rev. B **81**, 121302(R) (2010)]. We argue that the physics of the energy relaxation process at the QH edge may in fact be more rich, providing the possibility for discriminating between two physical pictures in experiment. Namely, using the recently proposed nonequilibrium bosonization technique [I. P. Levkivskyi *et al.*, Phys. Rev. Lett. **103**, 036801 (2009)], we evaluate the electron distribution function and find that the initial "double-step" distribution created at a QPC evolves through several intermediate asymptotics before reaching eventual equilibrium state. At short distances, the distribution function is found to be asymmetric due to non-Gaussian current noise effects. At larger distances, where noise becomes Gaussian, the distribution function acquires symmetric Lorentzian shape. Importantly, in the regime of low QPC transparencies T, the width of the Lorentzian scales linearly with T, in contrast to the case of equilibrium Fermi distribution, the width of which scales as $\sqrt{T}$. Therefore, we propose to do measurements at low QPC transparencies. We suggest that the missing energy paradox may be explained by the nonlinearities in the spectrum of edge states.

DOI: 10.1103/PhysRevB.85.075309 PACS number(s): 73.23.−b, 03.65.Yz, 85.35.Ds

I. INTRODUCTION

A two-dimensional electron gas (2DEG) in strong perpendicular magnetic field exhibits the regime of quantum Hall (QH) effect.[1] One of the peculiar phenomena specific to this regime is the appearance of one-dimensional (1D) *chiral* edge states, which are quantum analogs of skipping orbits. Recent extensive experimental studies[2–6] of these states have led to the emergence of a new field in condensed matter physics dubbed the electron optics. On the theoretical side, there are two main points of view on the physics of QH edge states. One group of theories[7] suggests that at integer values of the Landau-level filling factor, the edge excitations are free chiral *fermions*. The second group of theories is based on the concept of the edge magnetoplasmon picture.[8] The fundamental edge excitations in these theories are the charged and neutral collective *boson* modes.

The domain where these two approaches meet each other is the *low-energy* effective theory.[9] In the framework of this theory, both fermion and boson excitations are two forms of the same entity. Namely, they can be equivalently rewritten in terms of each other:

$$\psi(x,t) \sim \exp[i\phi(x,t)],$$

where $\psi(x,t)$ is the fermion field and $\phi(x,t)$ is the boson field. However, this transformation is highly nonlinear, and in the presence of strong Coulomb interaction, fermions are not stable and decay into the boson modes, which are the eigenstates of the edge Hamiltonian.

Results of tunneling spectroscopy experiments[10] reasonably agree with the free-electron description of edge states at integer filling factors. However, the first experiment on Aharonov-Bohm (AB) oscillations of a current through the electronic Mach-Zehnder (MZ) interferometer[2] has shown that the phase coherence of edge states is strongly suppressed at energies, which are inversely proportional to the interferometer's size. Moreover, several subsequent experiments on MZ interferometers at filling factor $\nu = 2$ have shown puzzling results on finite bias dephasing[3–6] theoretically studied in Refs. 11–15. Namely, the visibility of AB oscillations in these experiments is found to have a lobe-type pattern as a function of the applied voltage bias. Such results are difficult to explain in terms of the fermion picture, while they all follow naturally from the plasmon physics,[13] where the Coulomb interaction plays a crucial role. Thus, the boson picture of edge excitations might be more appropriate.

In contrast to the above-mentioned nonlocal experiments, some local measurements seem to be not able to differentiate between two physical pictures of edge states. For example, both theories predict Ohmic behavior of the tunneling current, unless it is renormalized by a nonlinear dispersion of plasmons. Moreover, the equilibrium distribution of the bosons is equivalent to that of fermions (see the demonstration of this fact in Sec. IV C). Therefore, it might be interesting to investigate nonequilibrium local properties of edge states.

Nonequilibrium behavior of 1D systems has been a subject of intensive theoretical[16] and experimental[17] studies for a long time. However, only recently has it become possible to measure an electron distribution at quantum Hall edge $f(\epsilon)$ as a function of energy ϵ with high precision.[18] The main idea of the experimental technique is to restore the function $f(\epsilon)$ by measuring the differential conductance $\mathcal{G}$ of tunneling between two edges through a single level in a quantum dot:

$$\mathcal{G}(\epsilon) \propto \partial f(\epsilon)/\partial\epsilon, \tag{1}$$

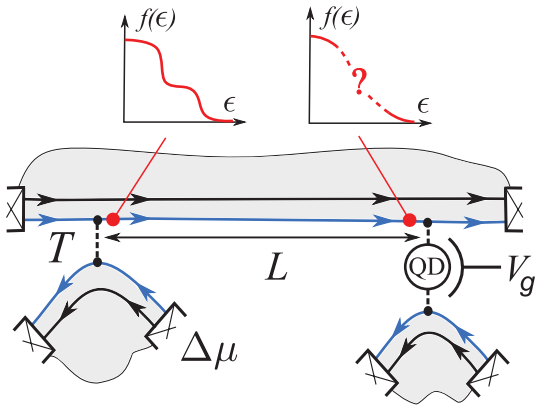

FIG. 1. (Color online) Schematics of the experiments (Refs. 18 and 19). The shaded region is filled by the 2D electron gas in the regime of the quantum Hall effect. At filling factor $\nu = 2$, there are two chiral edge states shown by the blue (the outer channel) and the black (the inner channel) lines. The QPC of the transparency T and biased with the voltage difference $\Delta\mu$ injects electrons into the outer channel, and thus creates a nonequilibrium electron distribution. After the propagation along the QH edge, the distribution is detected at distances L from the source with the help of a quantum dot with a single level controlled by the gate voltage V_g.

where ϵ is the energy of the quantum-dot level, controlled by the gate voltage V_g. This technique has been used in experiments[19] in order to investigate the energy relaxation at QH edge states at filling factor $\nu = 2$. The schematics of these experiments is shown in Fig. 1. The main result is that the electron distribution relaxes toward local equilibrium Fermi distribution, and the energy splits equally between the two edge channels.

The first theoretical models, based on the fermion picture[20] and on the plasmon approach,[21] have come qualitatively to *identical* conclusions. Namely, both works predict equal distribution of the energy between the edge channels, in agreement with the experimental findings. In other words, based on the results of Refs. 20 and 21 alone, the experimentalists are not able[19] to discriminate between two alternative descriptions of the physics of QH edge. Thus, it seems to be important and timely to reanalyze the problem of the energy relaxation at the QH edge in order to make new, model-specific and distinct predictions that can be verified experimentally. This is exactly the purpose of this work.

Here, we show that the Coulomb interaction strongly affects the spectrum of collective edge excitations and leads to the formation of charged and dipole plasmons modes, which propagate with different velocities.[22] They carry away the energy of electrons injected through the QPC and equally distribute it between edge channels at distances L_{ex} from the QPC. In addition to this observation, which agrees with findings of previous works,[20,21] we stress that the same process splits the wave packets of injected electrons and leads to strong coupling of electrons to the noise of the QPC current. The regime of weak injection, i.e., when the transparency of the QPC is small $T \ll 1$, deserves a special consideration. In this regime, the current noise at relevant time scales becomes Markovian and, as a result, the function $-\partial f(\epsilon)/\partial\epsilon$ acquires a Lorentzian shape. (This effect resembles a well-known phenomenon of the homogeneous level broadening.) Interestingly, the width of the Lorentzian scales as $T\Delta\mu$ at small T, where $\Delta\mu$ is the voltage bias applied to a QPC. In contrast, the width of the eventual equilibrium Fermi distribution of thermalized electrons scales as $\sqrt{T}\Delta\mu$. If thermalization takes place at longer distances $L_{eq} \gg L_{ex}$, then the intermediate regime described here may be observed in experiment with a weak injection. This would indicate that interactions strongly affect the physics at the edge and that the fermion picture becomes *inappropriate*.

In order to theoretically describe the experiments[19] and to quantitatively elaborate the physical picture, we use the *nonequilibrium* bosonization technique, which has been introduced in our previous work.[23] The main idea of this approach is based on the fact that in a 1D chiral system, one can find a nonequilibrium density matrix by solving equations of motion for plasmons with nontrivial boundary conditions. Then, one can rewrite an average over the nonequilibrium state of an interacting system in terms of the full counting statistics (FCS) generators[24] of the current at the boundary. In the situation considered in this paper, because of chirality of QH edge states, interactions do not affect the transport through the QPC alone. This leads to a great simplification because, in the Markovian limit, the FCS generator for free electrons is known.[24]

The structure of the paper is following: In Sec. II, we describe the nonequilibrium bosonization technique in some details. Next, we use this technique in Sec. III in order to find the electron correlation function for different distances from the QPC. Finally, we use these results to find the electron distribution function in Sec. IV, and present our conclusions in Sec. VI. Several important technical steps and the phenomena resulting from the nonlinearity of the spectrum of plasmons are described in Sec. V and the Appendices.

II. NONEQUILIBRIUM BOSONIZATION

We note that the relevant energy scales (voltage bias, temperature, etc.) in recent mesoscopic experiments with the QH edge states[3–6,18] are much smaller than the Fermi energy. Therefore, it is appropriate to use the low-energy effective theory[9] of the QH edge. One of the advantages of this theory is that it allows us to take into account strong Coulomb interactions in a straightforward way.[13] However, an additional complication arises from the fact that in experiments,[18,19] the injection into one of the two edge channels creates a strongly nonequilibrium state. We, therefore, start by recalling in this section the method of nonequilibrium bosonization, proposed earlier in Ref. 23, which is suitable for solving the type of a problem that we face. Throughout the paper, we set $e = \hbar = 1$.

A. Fields and Hamiltonian

According to the effective theory of QH edge,[9] the collective fluctuations of the charge densities $\rho_\alpha(x)$ of the two edge channels, $\alpha = 1,2$, at filling factor $\nu = 2$ are the only relevant degrees of freedom at low energies. These charge densities may be expressed in terms of the *chiral* boson fields $\phi_\alpha(x)$,

$$\rho_\alpha(x) = (1/2\pi)\partial_x\phi_\alpha(x), \tag{2}$$

which satisfy the following commutation relations:

$$[\phi_\alpha(x),\phi_\beta(y)] = i\pi\delta_{\alpha\beta}\,\mathrm{sgn}(x-y). \tag{3}$$

The vertex operator

$$\psi_\alpha(x) = \frac{1}{\sqrt{a}}\,e^{i\phi_\alpha(x)} \tag{4}$$

annihilates an electron at point x in the edge channel α. The constant a in the prefactor is the ultraviolet cutoff, which is not universal and will be omitted and replaced by other normalizations. One can easily check, with the help of the commutation relations (3), that the operators (4) indeed create a local charge of the value 1 at point x, and satisfy fermionic commutation relations.

Close to the Fermi level, the spectrum of electrons may be linearized; therefore, the free-fermion part $\mathcal{H}_0$ of the total QH edge Hamiltonian $\mathcal{H} = \mathcal{H}_0 + \mathcal{H}_{\rm int}$ takes the following form:

$$\mathcal{H}_0 = -iv_F\sum_\alpha\int dx\,\psi_\alpha^\dagger\partial_x\psi_\alpha, \tag{5}$$

where the bare Fermi velocity v_F is assumed to be the same for electrons at both edge channels. The second contribution to the edge Hamiltonian describes the density-density Coulomb interaction

$$\mathcal{H}_{\rm int} = (1/2)\sum_{\alpha,\beta}\iint dx\,dy\,U_{\alpha\beta}(x-y)\rho_\alpha(x)\rho_\beta(y), \tag{6}$$

which is assumed to be screened at distances d smaller than the characteristic length scale L in experiments,[3–6,18,19] i.e., $L \gg d$. Therefore, we may write

$$U_{\alpha\beta}(x-y) = U_{\alpha\beta}\delta(x-y). \tag{7}$$

Screening may occur due to the presence of either a back gate or several top gates. We show in the following that the assumption (7) results in the linear spectrum of charge excitations. This approximation seems to be reasonable, agrees well with some experimental observations such as an Ohmic behavior of the QPC conductance at low voltage bias, and eventually does not strongly affect our main results. Nevertheless, we relax this assumption and investigate the effects of weak and strong nonlinearities in the spectrum of charge excitations.

After taking into account the relations (2) and (4) and applying the point-splitting procedure, we arrive at the edge Hamiltonian of the quadratic form in boson fields

$$\mathcal{H} = \frac{1}{8\pi^2}\sum_{\alpha,\beta}V_{\alpha\beta}\int dx\,\partial_x\phi_\alpha(x)\partial_x\phi_\beta(x), \tag{8}$$

which nevertheless contains free-fermion contribution as well as the Coulomb interaction potential

$$V_{\alpha\beta} = 2\pi v_F\delta_{\alpha\beta} + U_{\alpha\beta}. \tag{9}$$

Equations (3), (4), (8), and (9) complete the description of the QH edge at low energies.

The experimentally found[18,19] electron distribution function at the outmost QH edge channel is given by the expression

$$f(\epsilon) = \int dt\,e^{-i\epsilon t}\langle\psi_1^\dagger(L,t)\psi_1(L,0)\rangle. \tag{10}$$

By rewriting this expression via the boson fields, we finally obtain

$$f(\epsilon) = \int dt\,e^{-i\epsilon t}K(t), \tag{11a}$$

$$K(t) = \langle e^{-i\phi_1(L,t)}e^{i\phi_1(L,0)}\rangle. \tag{11b}$$

where we have introduced the electron correlation function K, evaluated at coincident points at distance L from the QPC. The proportionality coefficient in Eq. (11b) may be corrected later from the condition that $f(\epsilon)$ takes a value 1 for energies well below the Fermi level (see, however, the discussion in Sec. V for further details). In equilibrium, in order to evaluate the correlation function on the right-hand side of this equation, one may now follow a standard procedure[25] of imposing periodic boundary conditions on the boson fields and diagonalizing the Hamiltonian (8). In our case, however, the average in (11) has to be taken over a *nonequilibrium* state created by a QPC. Attempting to express such a state entirely in terms of bosonic degrees of freedom is a complicated, and not a best, way to proceed. We circumvent this difficulty by applying a nonequilibrium bosonization technique proposed in our earlier work.[23] This technique is outlined in the following in some detail.

B. Equations of motion, boundary conditions, and FCS

The Hamiltonian (8), together with the commutation relations (3), generates equations of motion for the fields ϕ_α, which have to be complemented with boundary conditions[26]

$$\partial_t\phi_\alpha(x,t) = -\frac{1}{2\pi}\sum_\beta V_{\alpha\beta}\partial_x\phi_\beta(x,t), \tag{12a}$$

$$\partial_t\phi_\alpha(0,t) = -2\pi j_\alpha(t). \tag{12b}$$

The last equation follows from the charge continuity condition $\partial_t\rho_\alpha + \partial_x j_\alpha = 0$ and the definition (2). Thus, the operator $j_\alpha(t)$ describes a current through the boundary $x = 0$ in the channel α. For convenience, we place a QPC in the outer channel $\alpha = 1$ right before the boundary, so that the operator $j_1(t)$ describes an outgoing QPC's current.

The key idea of the nonequilibrium bosonization approach is to replace the average in Eq. (11) by the average over temporal fluctuations of currents j_α, the statistics of which is assumed to be known. Indeed, although in general the fields ϕ_α influence fluctuations of the currents j_α, leading to such effects as the dynamical Coulomb blockade[27] and cascade corrections to noise,[28] in the case of chiral fields describing QH edge states, no back-action effects arise.[11,13] As a consequence, at integer filling factors, the electron transport through a single QPC is not affected by interactions, which seems to be an experimental fact.[6,18] Therefore, by solving Eqs. (12), one may express the correlation functions of the fields ϕ_α in terms of the generator of FCS (Ref. 24):

$$\chi_\alpha(\lambda,t) = \langle e^{i\lambda Q_\alpha(t)}e^{-i\lambda Q_\alpha(0)}\rangle. \tag{13}$$

Here, averaging is taken over *free* electrons, and the operators

$$Q_\alpha(t) = \int_{-\infty}^{t}dt'\,j_\alpha(t') \tag{14}$$

may be viewed as a total charge in the channel α to the right of the boundary at $x = 0$.

To prove the connection of the electron correlations in (11) to the generating functions (13), we come back to the discussion of the interaction effects, which are in fact encoded in a solution of the equations of motion (12a). The long-range character of the Coulomb interaction leads to the logarithmic dispersion in the spectrum of collective charge excitations, the physical consequences of which are discussed in Secs. IV and V. For a moment, to simplify equations (12a), we have assumed screening of the Coulomb potential at distances d shorter than the characteristic length scale $v_F/\Delta\mu$, which is of the order of few microns in recent experiments. Nevertheless, it is very natural to assume that the screening length d is much larger than the distance a between edge channels $d \gg a$, which does not exceed a few hundred nanometers. Therefore, one can write

$$U_{\alpha\beta} = \pi u, \quad u/v_F \sim \ln(d/a) \gg 1, \tag{15}$$

i.e., the in-channel interaction strength is approximately equal to the intrachannel. As a result, the spectrum of collective charge excitations splits into two modes: a fast charged mode $\tilde{\phi}_1$ with the speed u and a slow dipole mode $\tilde{\phi}_2$ with the speed $v \simeq v_F$.

It is important to stress that the condition $d \gg a$, leading to (15), results in a sort of universality: the solution of equations of motion (12a) in terms of the charged and dipole mode

$$\phi_1(x,t) = \frac{1}{\sqrt{2}}[\tilde{\phi}_1(x-ut) + \tilde{\phi}_2(x-vt)], \tag{16a}$$

$$\phi_2(x,t) = \frac{1}{\sqrt{2}}[\tilde{\phi}_1(x-ut) - \tilde{\phi}_2(x-vt)] \tag{16b}$$

is only weakly sensitive to perturbations of our model, in particular to those that account for different bare Fermi velocities of edge channels and slightly different interaction strengths.

By applying now boundary conditions (12b) to the result (16), we finally solve equations of motion in terms of the boundary currents:

$$\phi_1(x,t) = -\pi \int_{-\infty}^{t_u} dt'[j_1(t') + j_2(t')] - \pi \int_{-\infty}^{t_v} dt'[j_1(t') - j_2(t')], \tag{17a}$$

$$\phi_2(x,t) = -\pi \int_{-\infty}^{t_u} dt'[j_1(t') + j_2(t')] + \pi \int_{-\infty}^{t_v} dt'[j_1(t') - j_2(t')], \tag{17b}$$

where we have introduced notations

$$t_u = t - x/u, \quad t_v = t - x/v. \tag{18}$$

Finally, using the definition (14), we arrive at the solution in the compact form

$$\phi_1(x,t) = -\pi[Q_1(t_u) + Q_2(t_u) + Q_1(t_v) - Q_2(t_v)], \tag{19}$$

and to a similar expression for the inner channel. The physical meaning of this result is rather simple: when charges are injected into the channel $\alpha = 1$ and 2, they excite charged and dipole modes (note the minus sign in the fourth term on the right-hand side), which have different propagation speeds u and v. As a result, these charges arrive at the observation point x with different time delays x/u and x/v, and make a contribution to the field ϕ_1 at different times (18).

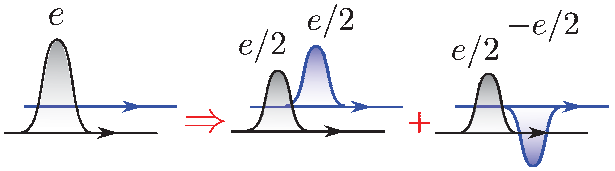

FIG. 2. (Color online) Schematic illustration of the Coulomb interaction effect at the QH edge at filling factor $\nu = 2$. The electron wave packet of the charge e created in the outer edge channel (black, lower line) decays into two eigenmodes of the Hamiltonian (8), the charged and dipole mode, which propagate with different speeds and carry the charge $e/2$ in the outer channel. As a result, the wave packets do not overlap at distances larger than their width, and contribute independently to the electron correlation function with the coupling constant $\lambda = \pi$ (Ref. 29). A similar situation arises when an electron is injected in the inner channel (blue, upper line), however, in this case the charged and dipole states carry opposite charges at the outer channel. Thus, there are four independent contributions to the correlation function in the outer edge channel.

When substituting this result into the correlation function in Eq. (11b), one may use the statistical independence of the current fluctuations at different channels and split the exponential functions accordingly:

$$K(t) = \left\langle e^{i\pi[Q_1(t_u)+Q_1(t_v)]} e^{-i\pi[Q_1(t_u-t)+Q_1(t_v-t)]} \right\rangle \times \left\langle e^{i\pi[Q_2(t_u)-Q_2(t_v)]} e^{-i\pi[Q_2(t_u-t)-Q_2(t_v-t)]} \right\rangle. \tag{20}$$

In the rest of the paper, we will be interested in the correlation function at relatively long distances $L \gg v\tau_c$, where $\tau_c \simeq 1/\Delta\mu$ is the correlation time of fluctuations of the current through a QPC. (We show below that at this length scale, the energy exchange between two channels takes place.) In this case, the partitioned charges Q_α, taken at different times t_u and t_v, are approximately not correlated, as illustrated in Fig. 2. This assumption is quite intuitive and may be easily checked using Gaussian approximation. We, finally, arrive at the following important result:

$$K(t) = \chi_1^2(\pi,t)\chi_2(-\pi,t)\chi_2(\pi,t), \tag{21}$$

i.e., the electronic correlation function (20) may indeed be expressed in terms of the FCS generator (13).

III. ELECTRON CORRELATION FUNCTION

The expression (21) presents formally a full solution of the problem of evaluation of an electron correlation function. Generators of the FCS for free electrons in this expression, defined as (13), may be represented as a determinant of a single-particle operator,[24] and eventually evaluated, e.g., numerically. However, a further analytical progress is possible in a number of situations, which are important for understanding physics of the energy relaxation processes. In particular, we show in this section that for the case of equilibrium fluctuations of the boundary currents, the correlation function (21) as well as

the electron distribution function (11) acquire an equilibrium free-fermionic form. The electron correlation function may also be found analytically away from equilibrium for the case of a Gaussian noise. Interestingly, in the short-time limit $t \ll 1/\Delta\mu$, the main contribution to the correlation function comes from zero-point fluctuations of boundary currents, and it behaves as a free-fermion correlator, i.e., it scales as $1/t$. In the long-time limit $t \gg 1/\Delta\mu$, the nonequilibrium zero-frequency noise dominates, and the electron correlation function decays exponentially with time. This is exactly the limit where a non-Gaussian Markovian noise should also be taken into account.

A. Gaussian noise

In the context of the noise detection physics,[24,30] the dimensionless counting variable λ in the expression (21) for the FCS generator plays the role of a coupling constant. Typically, it is small, $\lambda \ll 1$, so that the contributions of high-order cumulants of current noise to the detector signal are negligible.[30] In contrast, in the physical situation that we consider in this paper, $\lambda = \pm\pi$, implying that the shape of the distribution function may be strongly affected by high-order current cumulants. Nevertheless, it is instructive to first consider Gaussian fluctuations, simply truncating the cumulant expansion at second order in λ. In this case, the correlation function (20) may be evaluated exactly. There are many reasons for starting the analysis from considering an example of a Gaussian noise: First of all, in equilibrium, the current fluctuations in a chiral 1D system are always Gaussian. Second, as we show in Appendix C, the dispersion of the charged and dipole modes leads to a suppression of higher-order cumulants at large distances L. Finally, on the Gaussian level, it is easier to investigate and compare contributions of zero-point fluctuations and of nonequilibrium noise to the electron correlation function.

Thus, by expanding the logarithm of the right-hand side of Eq. (13) to second order in λ and accounting for Eq. (14), we obtain

$$\ln[\chi_\alpha(\lambda,t)] = i\lambda\langle j_\alpha\rangle t - \lambda^2 J_\alpha(t). \tag{22}$$

Here, the Gaussian contribution of current fluctuations $\delta j_\alpha(t) \equiv j_\alpha(t) - \langle j_\alpha\rangle$ is given by the following integral:

$$J_\alpha(t) = \frac{1}{2\pi}\int \frac{d\omega\, S_\alpha(\omega)}{\omega^2+\eta^2}(1-e^{-i\omega t}), \quad \eta \to 0 \tag{23}$$

where the nonsymmetrized noise power spectrum is defined as

$$S_\alpha(\omega) = \int dt\, e^{i\omega t}\langle \delta j_\alpha(t)\delta j_\alpha(0)\rangle. \tag{24}$$

In what follows, we apply this result for the evaluation of the electron correlation function in the case of equilibrium boundary conditions and in the case of a Gaussian noise far away from equilibrium.

1. Equilibrium boundary conditions

One may propose the following simple test of the nonequilibrium bosonization method: Let us consider an infinite QH edge. In equilibrium, the charge densities and edge currents exhibit thermal fluctuations. This is the case, in particular, for the currents j_α through the cross section $x = 0$, which are considered to be boundary conditions for the field ϕ_α in our theory. Therefore, one may evaluate the electron correlation function using these boundary conditions and compare it with the result of the standard equilibrium bosonization technique,[25] applied to a chiral 1D system.[13]

In equilibrium, $\langle j_\alpha\rangle = 0$. The current noise power spectrum is given by the fluctuation-dissipation relation[31]

$$S_\alpha(\omega) \equiv \int dt\, e^{i\omega t}\langle j_\alpha(t) j_\alpha(0)\rangle = \frac{1}{2\pi}\frac{\omega}{1-e^{-\beta\omega}}. \tag{25}$$

By substituting this expression into Eq. (23), one obtains

$$\ln[\chi_\alpha(\lambda,t)] = -\frac{\lambda^2}{4\pi^2}\int \frac{d\omega}{\omega}\frac{1-e^{-i\omega t}}{1-e^{-\beta\omega}}. \tag{26}$$

This integral may be evaluated by expanding the integrand in Boltzmann factors $e^{\pm\beta\omega}$ and integrating each term. By substituting the result (for $\lambda = \pi$) into Eq. (21), we arrive at the following expression for the electron correlation function in the case of equilibrium boundary conditions:

$$K(t) \propto \frac{\beta^{-1}}{\sinh(\pi t/\beta)}, \tag{27}$$

which is, in fact, the equilibrium fermionic correlation function. The straightforward calculations of the integral (11a) give, naturally, the equilibrium distribution function $f_1(\epsilon) = 1/(1+e^{\beta\epsilon}) \equiv f_F(\epsilon)$, where we have fixed the normalization constant, as explained above. Thus, for chiral, interacting quasi-1D systems with linear spectrum equilibrium bosons also implies equilibrium distribution of fermions.

It is instructive to compare this result with the known expression for the electron correlation function at $\nu = 2$, found earlier in Ref. 13 with the help of the standard bosonization technique

$$K(t) = \beta^{-1}\left[\sinh\left(\frac{x-y-vt}{v\beta/\pi}\right)\sinh\left(\frac{x-y-ut}{u\beta/\pi}\right)\right]^{-1/2}. \tag{28}$$

For $x = y$, details of the interaction leading to wave-packet splitting (see Fig. 2) vanish, and one obtains the expression (27), thus validating our approach. Moreover, the free-fermionic character of the correlation function at coincident points (27) justifies the assumption underlying the nonequilibrium bosonization procedure that the FCS generators (13) may be taken as for free electrons.

2. Gaussian noise away from equilibrium

For a QPC far away from equilibrium, $\beta\Delta\mu \gg 1$, one may simply set the temperature to zero. Straightforward calculations based on the scattering theory[32] give the following result for the spectral density of noise (24) of a QPC:

$$S_\alpha(\omega) = S_{\rm q}(\omega) + R_\alpha T_\alpha S_{\rm n}(\omega), \tag{29}$$

where $T_\alpha = 1 - R_\alpha$ is the transparency of a QPC (i.e., the average occupation in the channel α), $S_{\rm q}(\omega) = (1/2\pi)\omega\theta(\omega)$ is the quantum, ground-state spectral function, and $S_{\rm n}(\omega) = \sum_\pm S_{\rm q}(\omega \pm \Delta\mu) - 2S_{\rm q}(\omega)$, is the nonequilibrium contribu-

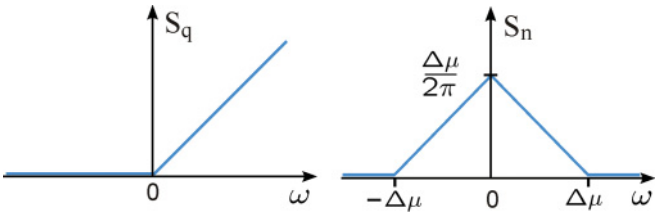

FIG. 3. (Color online) Two contributions to the spectral density of noise (29). Left panel: Quantum contribution $S_q(\omega)$ generated by the incoming Fermi sea. This contribution vanishes at low frequencies $S_q(0) = 0$, but dominates the behavior of the correlator (23) at short times $t\Delta\mu \ll 1$. Right panel: Nonequilibrium contribution $S_n(\omega)$ dominates at long times $t\Delta\mu \gg 1$, i.e., in the Markovian limit.

tion (see Fig. 3). Note that the noise power (29) differs from that for a nonchiral case.[30]

Evaluating the integral (23), we arrive at the following expression:

$$J_\alpha(t) = (1/4\pi^2)[\ln t + 2R_\alpha T_\alpha f(\Delta\mu t)], \tag{30}$$

where the logarithm of time originates from the quantum contribution S_q, and the dimensionless function $f(\Delta\mu t)$, describing nonequilibrium noise, is given by the integral

$$f(\Delta\mu t) = \int_0^1 ds\, \frac{1-s}{s^2}\,[1-\cos(\Delta\mu t s)]. \tag{31}$$

This function has a quadratic behavior $f(\Delta\mu t) \simeq (\Delta\mu t)^2/4$ at short times $\Delta\mu t \ll 1$, while in the long-time (Markovian) limit $\Delta\mu t \gg 1$, the dominant contribution to this function is linear in time: $f(\Delta\mu t) \simeq (\pi/2)|\Delta\mu t|$.

For the purpose of further analysis, we need the electron correlation function in the long-time limit. Taking into account that $\langle j_\alpha\rangle = \Delta\mu T_\alpha/2\pi$, we find the cumulant generating function

$$\ln[\chi_\alpha] = \frac{i\lambda}{2\pi}\Delta\mu T_\alpha t - \left(\frac{\lambda}{2\pi}\right)^2 (\ln t - \pi R_\alpha T_\alpha |\Delta\mu t|),\ \ \Delta\mu t \gg 1. \tag{32}$$

Finally, substituting this result into Eq. (21), and setting $T_1 = T$ and $T_2 = 1$ according to the situation shown in Fig. 1, we obtain the electron correlation function in the long-time limit:

$$K(t) \propto t^{-1} e^{i\Delta\mu T t - \pi RT\Delta\mu|t|/2},\quad \Delta\mu t \gg 1. \tag{33}$$

Note that the expression (33) contains the quantum contribution in the form of a single pole, as for free fermions, as well as the nonequilibrium contribution in the form of an exponential envelope, the width of which is determined by the noise power at zero frequency $S_1(0) = RT\Delta\mu/2\pi$. The phase shift of the correlator is determined by the "average" voltage bias $\langle\Delta\mu\rangle = \Delta\mu T$ of the incoming stream of electrons, diluted by the QPC. In the next section, we show that this mean-field-like effect of the dilution is strongly modified by a non-Gaussian component of noise.

B. Non-Gaussian Markovian noise

Here, we consider non-Gaussian noise and show that the contribution of high-order cumulants of current to the correlation function is not small. Note that the quantum ground-state part of the current noise S_q, which dominates at short times, is pure Gaussian. Therefore, the denominator in the expression (33) remains unchanged. In the long-time, Markovian limit, the dominant contribution to the FCS generator comes from the nonequilibrium part of noise, which, e.g., is described by S_n in Gaussian case. For a QPC, the Markovian FCS generator is given by the well-known expression[24] for a binomial process

$$\chi_1(\lambda,t) = (R + Te^{i\lambda})^N, \tag{34}$$

where $N = \Delta\mu t/2\pi$ is the total number of electrons that contribute to noise. By applying the analytical continuation $\lambda \to \pi$, we obtain

$$\ln[\chi_1(\pi,t)] = \frac{\Delta\mu t}{2\pi}[\ln|T-R| + i\pi\theta(T-R)]. \tag{35}$$

By substituting this expression to the correlation function (21), we arrive at the result

$$K(t) \propto t^{-1} e^{i\theta(T-R)\Delta\mu t + \ln|T-R|\Delta\mu|t|/\pi}, \tag{36}$$

where the imaginary part of the exponent determines the effective voltage bias, while the real part is responsible for dephasing.

Interestingly, at the point $T = 1/2$, the dephasing rate is divergent, and the effective voltage bias drops to zero abruptly for $T < 1/2$. It has been predicted in Ref. 23 that this behavior may lead to a phase transition in the visibility of Aharonov-Bohm oscillations in electronic Mach-Zehnder interferometers. We will argue in the following that no sharp transition arises in the electron distribution function. However, it leads to its strong asymmetry with respect to the average voltage bias $\langle\Delta\mu\rangle = T\Delta\mu$ of the outer channel.

IV. ELECTRON DISTRIBUTION FUNCTION

In this section, we use the results (27), (33), and (36) for the correlation function of electrons to evaluate and analyze the electronic distribution function. We start by noting that the experiments (Refs. 18 and 19) are done in a particular regime of strong partitioning $T \approx 0.5$ at the QPC injecting current to the channel $\alpha = 1$. This detail, which seems to be irrelevant from the first glance, is in fact of crucial importance. Indeed, as it follows from the expressions (33) and (36), the main contribution to the integral (11a) for the correlation function comes from times t of the order of the correlation time $\tau_c \simeq 1/\Delta\mu$, where our results based on the Markovian noise approximation are, strictly speaking, not valid. However, the numerical calculations show that the nonequilibrium distribution in this regime is very close to the equilibrium one. Therefore, the actual equilibration of electrons, which is reported in the experiment Ref. 18 to occur at distances $v/\Delta\mu$, may in fact take place at even longer distances $L_{eq} \gg v/\Delta\mu$ due to an unknown mechanism (not considered here).

Indeed, if the chiral Luttinger-liquid model considered in our paper is valid, then neither the strong interaction between electrons of two edges taken alone nor the weak dispersion of plasmons resulting from a long-range character of Coulomb interaction may lead to the equilibration because the systems remain integrable. Thus, it seems to be reasonable to assume that the equilibration length L_{eq} may indeed be

quite long. Therefore, in order to explore the physics of collective charge excitations at intermediate distances, we propose to consider a regime of weak injection at the QPC: $T \ll 1$. First, we note that in this case our results (33) and (36) may indeed be used to evaluate the electron distribution function because the main contribution to the integral (11a) arises from Markovian time scales. Second, and more importantly, in this regime the electron distribution function acquires a strongly nonequilibrium form and the width of the order of $T\Delta\mu$, which plays a role of the new energy scale. Moreover, the advantage of the weak injection regime is that it allows us to investigate a nontrivial evolution of the distribution function, which arises due to bosonic, collective character of excitations and goes via several well distinguishable steps.

A. Short distances

At distances of the order of the energy exchange length scale

$$L_{\rm ex} \equiv v/\Delta\mu, \tag{37}$$

the initial double-step distribution function is strongly perturbed by the interaction between channels. As we argued in Sec. II B, at distances $L \gg L_{\rm ex}$, the charged and dipole modes split and make independent contributions to the electron correlation function. Therefore, we may rely on the result (36). By applying the limit $T \ll 1$ to this expression and evaluating the Fourier transform, we find

$$-\frac{\partial f(\epsilon)}{\partial\epsilon} = \frac{\Gamma_{\rm ng}/\pi}{\epsilon^2+\Gamma_{\rm ng}^2}, \quad \Gamma_{\rm ng} = 2T\Delta\mu/\pi. \tag{38}$$

Here, the missing prefactor in the correlation function has been fixed by the requirement that $f(\epsilon) = 1$ at $\epsilon \to -\infty$. Thus, we conclude that the energy derivative of the distribution function acquires a narrow Lorentzian peak, which is shifted with respect to the average bias $\langle\Delta\mu\rangle = T\Delta\mu$ and centered at $\epsilon = 0$. The last effect is a unique signature of the non-Gaussian character of noise. Because of the electron-hole symmetry of the binomial process, in the limit $R \ll 1$ the Lorentzian peak obviously has a width $\Gamma_{\rm ng} = 2R\Delta\mu/\pi$ and centered at $\epsilon = \Delta\mu$.

We stress again that the result (38) holds only for small enough energies close to the Fermi level, namely, for $|\epsilon| < \Delta\mu$, where the main contribution arises from the noise in the Markovian limit. In fact, the result (38) fails at large energies in a somewhat nontrivial way. Namely, it is easy to see that any electron distribution function has to satisfy the sum rule

$$\langle\Delta\mu\rangle \equiv \epsilon_0 + \int_{\epsilon_0}^{\infty} d\epsilon\, f(\epsilon) = -\int_{-\infty}^{\infty} d\epsilon\, \epsilon\, \partial f(\epsilon)/\partial\epsilon, \tag{39}$$

where ϵ_0 is the cutoff well below the Fermi level, and the "average" bias $\langle\Delta\mu\rangle = T\Delta\mu$ in the case of linear dispersion of plasmons. This sum rule simply expresses the requirement of the conservation of the charge current and implies a certain amount of asymmetry in the distribution function. In the present case, such an asymmetry arises in the power-law tails of the function $-\partial f(\epsilon)/\partial\epsilon$ and originates from quantum nonequilibrium noise. It can be seen in Fig. 4.

Moreover, at energies of the order of $\Delta\mu$, the power-law behavior of the function (38) has to have a cutoff because the QPC does not provide energy much larger than the voltage bias. Quantitatively, this follows from the conservation of the energy. We demonstrate in the following that for the system with linear dispersion of plasmons, the heat flux in the outer channel can be written entirely in terms of the single-electron distribution function (in units $e = \hbar = 1$)

$$I_{\rm m} = (1/2\pi)\int d\epsilon\, \epsilon\, [f(\epsilon) - \theta(\langle\Delta\mu\rangle - \epsilon)], \tag{40}$$

as in the case of free electrons. We use the subscript "m" in order to emphasize the fact that it is this quantity that has been measured in the experiment (Ref. 19). In Sec. V, we show that at distances $L \gg L_{\rm ex}$ the total heat flux injected at a QPC splits equally between two edge channels; therefore, integrating Eq. (40) by parts and substituting the heat flux for a double-step distribution, we obtain

$$I_{\rm m} = -\frac{(T\Delta\mu)^2}{4\pi} - \frac{1}{4\pi}\int d\epsilon\, \epsilon^2 \frac{\partial f(\epsilon)}{\partial\epsilon} = \frac{TR(\Delta\mu)^2}{8\pi} \tag{41}$$

for $L \gg L_{\rm ex}$. One can see from Eq. (38) that indeed the power-law behavior has to have a cutoff at $|\epsilon| \sim \Delta\mu$. We stress, however, that this summation rule is less universal than the one given by Eq. (39) because it accounts only for a single-particle energy of electrons and fails in the case of a nonlinear spectrum of plasmons, considered in Sec. V in detail.

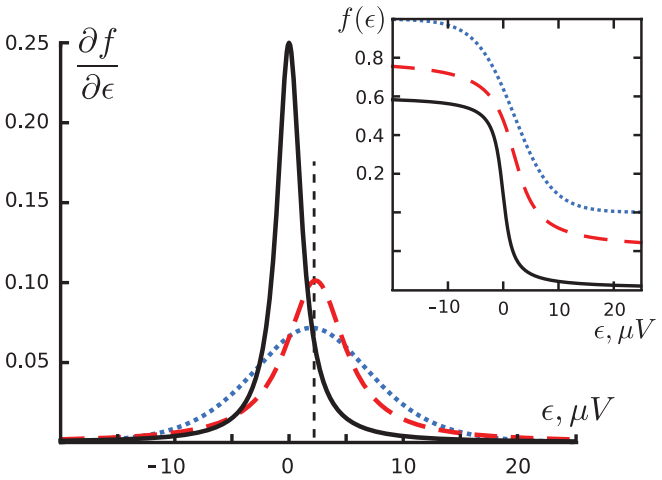

FIG. 4. (Color online) Energy derivative of the electron distribution function $-\partial f/\partial\epsilon$ is shown for different distances L from the QPC injecting current. The transparency of the QPC is set to $T = 0.05$ and voltage bias is $\Delta\mu = 40\ \mu$V. Black line: $-\partial f(\epsilon)/\partial\epsilon$ for short distances $L_{\rm ex} \ll L \ll L_{\rm g}$, so that the noise is non-Gaussian (38). Red, dashed line: $-\partial f(\epsilon)/\partial\epsilon$ for intermediate distances $L_{\rm g} \ll L \ll L_{\rm eq}$, where the noise is Gaussian (44). Blue, dotted line: The derivative of the Fermi distribution function at the temperature given by Eq. (47). The dashed line is a guide for the eyes at the energy equal to the effective voltage bias $\langle\Delta\mu\rangle = T\Delta\mu = 2\,\mu V$. Inset: The same distribution functions are shown in the integrated form. They are shifted vertically by 0.2 intervals for clarity.

B. Intermediate distances

So far, we have considered the case of a linear spectrum of plasmons. This is a reasonable assumption, taking into account

the fact that nonlinear corrections in the spectrum of plasmons lead to a nonlinear corrections in the Ohmic conductance of a QPC. However, the experiments (Refs. 18 and 19) seem to be done in the Ohmic regime. Nevertheless, even in the case of a weak nonlinearity in the spectrum of the the both modes of the sort[33]

$$k_j(\omega) = \omega/v_j + \gamma_j \omega^2 \mathrm{sign}(\omega), \quad v_1 = u,\ v_2 = v, \tag{42}$$

barely seen in the conductance of a QPC, an intermediate length scale L_g may arise at which high-order cumulants of current are suppressed, and the noise becomes effectively Gaussian. This situation occurs when the wave packets of the original width $v/(T\Delta\mu)$ overlap. A simple estimate using the nonlinear correction (42) gives the length scale

$$L_g = 1/\gamma(T\Delta\mu)^2, \quad \gamma \equiv \min(\gamma_j). \tag{43}$$

We support this conclusion by rigorous calculations in Appendix C.

The nonlinearity in the spectrum is weak if $\gamma v T \Delta\mu \ll 1$. This implies that $L_g \gg L_{ex}$, and leads to the possibility to observe non-Gaussian effects at distances $L_{ex} \ll L \ll L_g$ discussed in the previous section. Obviously, the same requirement also guarantees that dispersion corrections to the Ohmic conductance of a QPC are small. This allows us to neglect corrections to the quantum part of the electron correlation function and to use the result (33) for a Gaussian noise. By substituting this result to Eq. (11a), we obtain

$$-\frac{\partial f(\epsilon)}{\partial \epsilon} = \frac{\Gamma_{ng}/\pi}{(\epsilon - \langle\Delta\mu\rangle)^2 + \Gamma_g^2}, \quad \Gamma_g = \pi T \Delta\mu/2 \tag{44}$$

in the case $L_g \ll L \ll L_{eq}$. One can see that the width of the function (44) is almost twice as large compared to that in the function (38). Moreover, the function (44) satisfies the sum rule (39). Therefore, we do not expect any asymmetry in the high-energy tails of this function, in contrast to the situation with the non-Gaussian noise. The comparison of distribution functions in these two regimes is shown in Fig. 4.

So far, we have considered a situation where both charged and dipole modes are dispersive. If for some reason the dispersion of one of the modes is negligible, then higher-order cumulants are suppressed only by a factor of 2. The derivative of the electron distribution function in this situation is given by the Lorentzian

$$\frac{\partial f(\epsilon)}{\partial \epsilon} = \frac{(\Gamma_{ng} + \Gamma_g)/2\pi}{(\epsilon - \langle\Delta\mu\rangle/2)^2 + (\Gamma_{ng} + \Gamma_g)^2/4} \tag{45}$$

centered at $\langle\Delta\mu\rangle/2 = \Delta\mu T/2$ with the width $(\Gamma_{ng} + \Gamma_g)/2 = (1/\pi + \pi/4)\Delta\mu T$. This is because one mode brings only the Gaussian component of the Markovian noise, while the other one brings full non-Gaussian noise.

C. Long distances

Next, we consider the distribution function at long distances $L \gg L_{eq}$ after the equilibration takes place. The temperature of the eventual equilibrium distribution may be found from the conservation of energy. In the next section, we show that the heat flux produced at QPC splits equally between two edge states. In the situation of linear dispersion, the distribution function acquires the form

$$f(\epsilon) = \frac{1}{1 + e^{(\epsilon - \langle\Delta\mu\rangle)/\Gamma_{eq}}}. \tag{46}$$

The possibility of such an equilibration process is suggested by the fact that the equilibrium distribution of bosons implies the equilibrium distribution for electrons, as has been shown in Sec. III A 1. Obviously, the distribution (46) satisfies the sum rule (39), while the energy conservation condition (41) may now be used in order to find the effective temperature:

$$\Gamma_{eq} = \sqrt{3T/2\pi^2}\Delta\mu, \tag{47}$$

where we have used $T \ll 1$.

We conclude that the width of the equilibrium distribution scales as $\sqrt{T}$, in contrast to the case of a nonequilibrium distribution at shorter distances from the current source, where it scales linear in T. Therefore, if T is small, equilibrium and nonequilibrium distributions may easily be distinguished, as illustrated in Fig. 4. In the situation where the dispersion can not be neglected, the equilibrium distribution of fermions is not given by the Fermi function (46). This situation deserves a separate consideration, which is provided in the next section.

V. MEASURED AND TOTAL HEAT FLUXES

We have seen that in the case of weakly dispersive plasmons $\gamma v T \Delta\mu \ll 1$, the nonlinearity in the spectrum leads to the suppression of high-order cumulants of current noise at relatively long distances, which strongly affects the distribution function. On the other hand, the direct contribution of the nonlinear correction in the spectrum to local physical quantities, such as the QPC conductance and the heat flux, is small and has been so far neglected. Nevertheless, it may manifest itself experimentally in a quite remarkable way. In this section, we show that the nonlinearity in the the plasmon spectrum contributes differently to the measured heat flux (40) and to the actual heat flux expected from the simple evaluation of the Joule heat. As we demonstrate below, this may, under certain circumstances, explain the missing energy paradox in the experiment Ref. 19.

We start by noting that the measured flux (40) at the distance L from the QPC may be expressed entirely in terms of the excess noise spectrum $\mathbb{S}_\alpha(\omega) \equiv S_\alpha(\omega) - (1/2\pi)\omega\theta(\omega)$ of edge channels right after the QPC, where $S_\alpha(\omega)$ is defined in (24). Namely, in Appendix B, we derive the following result:

$$I_m(L) = \frac{1}{4}\int_{-\infty}^{\infty} d\omega \{\mathbb{S}_1(\omega)[1 + \cos(\Delta k L)] + \mathbb{S}_2(\omega)[1 - \cos(\Delta k L)]\}, \tag{48}$$

where $\Delta k \equiv k_1(\omega) - k_2(\omega)$ and $k_j(-\omega) = -k_j(\omega)$. Importantly, this result holds for an arbitrary nonlinear spectrum $k_j(\omega)$ of the charged and dipole modes, and for a non-Gaussian noise in general, i.e., high-order cumulants simply do not contribute.

One can easily find two important limits of Eq. (48): for $L = 0$, we immediately obtain an expected result

$$I_m(0) = \frac{1}{2}\int_{-\infty}^{\infty} d\omega\, \mathbb{S}_1(\omega), \tag{49}$$

while at $L \to \infty$ the cosine in (48) acquires fast oscillations, and we get

$$I_{\rm m}(\infty) = \frac{1}{4}\int_{-\infty}^{\infty} d\omega[\mathbb{S}_1(\omega) + \mathbb{S}_2(\omega)]. \tag{50}$$

To be more precise, this happens at $L \gg L_{\rm ex} = v/\Delta\mu$. At zero temperature, $\mathbb{S}_2$ vanishes and the single-electron heat flux $I_{\rm m}$, created at the QPC, splits equally between edge channels: $I_{\rm m}(\infty) = I_{\rm m}(0)/2$. Note also that in the case of linear dispersion $\mathbb{S}_\alpha = T_\alpha R_\alpha S_{\rm n}$, where $S_{\rm n}$ is shown in Fig. 3.

In the next step, we rewrite the same measured flux in terms of the plasmon distributions $n_j(k) = \langle \tilde{a}_j^\dagger(k)\tilde{a}_j(k)\rangle$ (see Appendix B):

$$I_{\rm m}(\infty) = \frac{1}{4\pi}\sum_j \int \frac{dk}{k}\,\omega_j^2(k) n_j(k) + I_{\rm q}, \tag{51}$$

$$I_{\rm q} = \frac{1}{8\pi}\sum_j \int \frac{dk}{k}\left[\omega_j^2(k) - (v_j k)^2\right], \tag{52}$$

where $v_j = \partial\omega_j/\partial k$ are the plasmon speeds at $k = 0$. The term $I_{\rm q}$ is the contribution to the measured flux from quantum smearing of the zero-temperature electron distribution function $f_0(\epsilon)$ close to the Fermi level, which originates from a nonlinear dispersion of plasmons.

Here, an important remark is in order. The integral (52) may diverge at large k and has to be cut off at the upper limit. This is because there is no guarantee of the free-fermionic behavior of the correlator $K(t)$ at short times and of the zero-temperature electron distribution function $f_0(\epsilon)$ at large energies. Thus, the integral (40) has to be also cut off, which is what in fact is done in experiment. In contrast, the spectrum of plasmons is linear at small k, and thus the distribution function $f_0(\epsilon)$ has a free-fermionic behavior close to the Fermi level. Our definition of $I_{\rm q}$ corresponds to the normalization of $f_0(\epsilon)$ to have a discontinuity of the value -1 at $\epsilon = \langle\Delta\mu\rangle$. The experimentally measured $I_{\rm q}$ may differ from the one defined in (52) by a constant, which is, on the other hand, independent on the voltage bias $\Delta\mu$.

Next, we note that the actual total heat flux in the case of a nonlinear dispersion of plasmons acquires the completely different form[34]

$$I_{\rm h} = \frac{1}{2\pi}\sum_j \int dk \frac{\partial\omega_j}{\partial k}\omega_j(k)\, n_j(k), \tag{53}$$

and thus in general $I_{\rm m} \neq I_{\rm h}/2$, contrary to what has been assumed in the experiment Ref. 19. This may explain the missing energy paradox. Indeed, by assuming the low ω spectrum of the general form

$$k_j = \omega/v_j + \gamma_j\omega^{\ell_j}, \quad j = 1,2 \tag{54}$$

where γ_j are small, and equilibration of plasmons at $L \to \infty$, i.e., $n_j(k) = n_B(\omega_j/\Gamma_{\rm eq}) = 1/[\exp(\omega_j/\Gamma_{\rm eq}) - 1]$, we obtain the missing heat flux as

$$I_{\rm m} - I_{\rm q} - I_{\rm h}/2 = \sum_{j=1,2} c_j\gamma_j v_j \Gamma_{\rm eq}^{\ell_j+1}, \tag{55}$$

where the constants $c_j = (1/4\pi)\int dz\, z^{\ell_j+1} n_B(z)$ are of the order of 1. This result implies that experimentally, the missing heat flux may be found by investigating its bias dependence and the spectrum of plasmons.

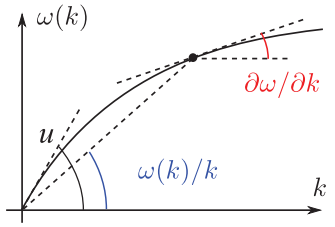

FIG. 5. (Color online) Typical spectrum of charged plasmon in the case of the Coulomb interaction screened at distances $d \ll 1/k$. This spectrum is concave, i.e., $\partial\omega/\partial k < \omega(k)/k$.

Let us consider an example where the dispersion of charged plasmon at small k arises from the screened Coulomb interaction[8]

$$\begin{aligned}\omega/k &= 2[\mathcal{K}_0(ka) - \mathcal{K}_0(kd)] \\ &= 2\,\ln(d/a) - (1/2)(kd)^2\ln(2/kd),\end{aligned} \tag{56}$$

where a is the high-energy cutoff, d is the distance to the gate, such as $ka \ll kd \ll 1$, and $\mathcal{K}_0$ is the MacDonald function. The low-k asymptotics of this spectrum is illustrated in Fig. 5. One can see that the spectrum is concave, so that in this case the measured heat flux (51) is larger than the half of the actual heat flux (53). In addition, the effect is weak, because $kd \sim 0.1$ in the experiment Ref. 19. Thus, the dispersion of the Coulomb interaction potential alone is not able to explain the missing flux paradox. Various mechanisms of convex dispersion are still possible and will be investigated elsewhere.

VI. CONCLUSIONS

Earlier theoretical works on quantum Hall edge states at integer filling factors may be divided into two groups: fermion-based and boson-based theories. Recent interference experiments suggest that the boson approach might be more appropriate for the description of the edge physics. However, both groups of theories give the same predictions for the local physical quantities at equilibrium. Moreover, the first theoretical works based on fermion[20] and boson[21] approaches and addressing the nonequilibrium local measurements have not been able to make qualitatively distinct predictions. In this paper, we show that it is nevertheless *possible* to test and differentiate between two approaches with the local nonequilibrium measurements.

We address recent experiments (Refs. 18 and 19) with quantum Hall edge states at filling factor 2, where an energy relaxation process has been investigated by creating a nonequilibrium state at the edge with the help of a QPC and reading out the electron distribution downstream using a quantum dot. We use the nonequilibrium bosonization approach[23] in order to describe the gradual relaxation of initially nonequilibrium, double-step electron distribution to its equilibrium form. In the framework of this approach, the nonequilibrium initial state is encoded in the boundary conditions for the equations of motions that depend on interactions. We show that the electrons excite two plasmons: fast charged and slow dipole modes. Thus, the electron correlation function (21) is expressed in terms of the four contributions, each having the form of the

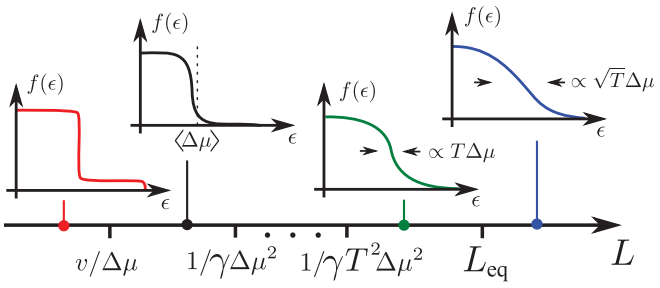

FIG. 6. (Color online) Different length scales for energy relaxation processes and corresponding distribution functions in each regime are schematically shown. Red curve: The initial double-step distribution function. Black curve: At distances $L \gg \Delta\mu/v$, the distribution function is strongly asymmetric with respect to the "average" bias $\langle\Delta\mu\rangle = T\Delta\mu$. Green curve: At distances $L \gg 1/\gamma(T\Delta\mu)^2$, the distribution function is a Lorentzian with the width that scales as $T\Delta\mu$. Blue curve: The final equilibrium Fermi function at large distances. For small transparencies, its width scales as $\sqrt{T}\Delta\mu$.

generator of FCS of free electrons with the coupling constant $\lambda = \pi$. By evaluating the Fourier transform of this function, we find the electron distribution function.

Before reaching eventual equilibrium form, the distribution function evolves via several steps, where its energy derivative acquires a Lorentzian shape:

$$\frac{\partial f(\epsilon)}{\partial\epsilon} = \frac{\Gamma/\pi}{(\epsilon-\epsilon_0)^2+\Gamma^2}, \quad |\epsilon| \lesssim \Delta\mu. \tag{57}$$

Here, the width Γ and centering ϵ_0 take different values in different regimes. Each of the regimes, summarized below and illustrated in Fig. 6, has its own dominant process:

(i) First, after tunneling through the QPC, electrons excite plasmons, which then split in two eigenmodes: one is charged fast mode with the speed u, and the other is slow dipole mode with the speed v. This process takes place at distances $L_{\rm ex} = v/\Delta\mu$, where $\Delta\mu$ is the voltage bias across the QPC. In this regime, Eq. (21) applies, which eventually leads to the the distribution (57) with the width $\Gamma = \Gamma_{\rm ng} = 2\Delta\mu T/\pi$, centered at $\epsilon_0 = 0$.

(ii) Next, a weak dispersion of plasmons, e.g., of the form $k = \omega/v + \gamma\omega^2{\rm sign}(\omega)$, leads to broadening of wave packets of the energy width ϵ and to their overlap. This process takes place at distances $L \gg 1/\gamma\epsilon^2$. As a result, high-order cumulants of the current injected at the QPC are suppressed at distances $L \gg L_{\rm g} = 1/\gamma(T\Delta\mu)^2$, the noise becomes Gaussian, and the derivative of the electron distribution function acquires the shape (57) with the width $\Gamma = \Gamma_{\rm g} = \pi\Delta\mu T/2$, centered at $\epsilon_0 = \Delta\mu T$.

(iii) A situation is possible where the dispersion of one mode, most likely of the charged mode, is much stronger than the dispersion of the second mode, i.e., $\gamma_1 \gg \gamma_2$. In this case, the previously described regime splits in two separate regimes. First, at distances $L = 1/\gamma_1(T\Delta\mu)^2$, the contribution of the charged mode to high-order cumulants of noise becomes suppressed, which leads to the distribution (57) with the parameters $\Gamma = (\Gamma_{\rm ng}+\Gamma_{\rm g})/2$ and $\epsilon_0 = \Delta\mu T/2$. Then, at longer distances $L = 1/\gamma_2(T\Delta\mu)^2$, the noise becomes fully Gaussian.

(iv) The interaction may lead to broadening of the wave packets, but they do not decay, which implies that the interaction alone does not lead to the equilibration. This means that a different, weaker process may lead to the equilibration at distances $L_{\rm eq}$ much longer than the above-discussed length scales. In the tunneling regime $T \ll 1$, the width of the eventual equilibrium distribution scales as $\sqrt{T}$, in contrast to the above regimes, where it scales as T. Thus, to observe the described variety of regimes, we propose to perform measurements at large voltage biases and low transparencies of the QPC utilized to inject electrons.

Finally, we suggest a possible explanation of the paradox of missing heat flux in the experiment Ref. 19. So far, we have summarized the effects of weak dispersion, which lead to the appearance of intermediate length scales. We have found that in the case of a strongly nonlinear dispersion of plasmons, the measured heat flux $I_{\rm m}$ in the outmost edge channel, experimentally determined with the procedure described by Eq. (40), is different from the actual heat flux per channel $I_{\rm h}/2$, defined by Eq. (53). The screened Coulomb interaction leads to a rather weak dispersion of the charged plasmon, and the effect is of the opposite sign because the spectrum in this case is concave. Nevertheless, other mechanisms of the convex dispersion are possible. They will be considered elsewhere.

ACKNOWLEDGMENTS

We would like to thank F. Pierre for the clarification of the experimental details and P. Degiovanni for fruitful discussions. This work has been supported by the Swiss National Science Foundation.

APPENDIX A: SOLUTION OF EQUATIONS OF MOTION

In this Appendix, we solve the equations of motion (12a) with the boundary conditions (12b) in the case of a potential $U_{\alpha\beta}(x-y)$ of a finite range, where the plasmon spectrum is nonlinear. For doing this, we first write the normal mode expansion for the edge boson fields as

$$\phi_\alpha(x) = \varphi_\alpha + 2\pi\cdot\pi_\alpha x + \sum_k \sqrt{\frac{2\pi}{kW}}[a_{\alpha k}e^{ikx} + a^\dagger_{\alpha k}e^{-ikx}]. \tag{A1}$$

We consider zero modes to be classical variable because the commutator $[\pi_\alpha,\varphi_\alpha] = i/W$ vanishes in the thermodynamic limit $W \to 0$. Then, we rewrite the operators $a_{\alpha k}$ in the new basis $\tilde a_{jk}$, which diagonalizes the edge Hamiltonian (8):

$$\tilde a_{jk}(t) = \tilde a_{jk}e^{-i\omega_j(k)t}, \tag{A2}$$

where $j = 1,2$ and $\omega_j(k)$ is the dispersion of the jth mode. In the case where the in-channel interaction strength is approximately equal to the intrachannel one, $U_{\alpha\beta}(x-y) \approx U(x-y)$, and the interaction is strong, $U(k) = \int dx\, e^{ikx}U(x) \gg 2\pi v_F$, the transformation to the new basis is simple and universal:

$$a_{1k}(t) = \frac{1}{\sqrt{2}}(\tilde a_{1k}e^{-i\omega_1(k)t} + \tilde a_{2k}e^{-i\omega_2(k)t}), \tag{A3a}$$

$$a_{2k}(t) = \frac{1}{\sqrt{2}}(\tilde a_{1k}e^{-i\omega_1(k)t} - \tilde a_{2k}e^{-i\omega_2(k)t}). \tag{A3b}$$

Then, $\omega_1(k) = k[v_F + U(k)/\pi]$ for the charged plasmon, and $\omega_2(k) = vk$ for the dipole mode, where $v \approx v_F$.

In the next step, we use the boundary conditions (12b) to connect the current operators to the operators (A2):

$$\tilde{a}_{1k} = \frac{i}{\omega_1}\frac{\partial\omega_1}{\partial k}\sqrt{\frac{\pi k}{W}}\,[j_1(\omega_1) + j_2(\omega_1)], \tag{A4a}$$

$$\tilde{a}_{2k} = \frac{i}{\omega_2}\frac{\partial\omega_2}{\partial k}\sqrt{\frac{\pi k}{W}}\,[j_1(\omega_2) - j_2(\omega_2)], \tag{A4b}$$

where $j_\alpha(\omega) = \int dt\, e^{i\omega t} j_\alpha(t)$, and we have used the obvious relation $j_\alpha(-\omega) = j_\alpha^\dagger(\omega)$. Finally, substituting relations (A4) into Eq. (A3a) and then to the expansion (A1), we find the solution of the equations of motion for the boson fields. In particular,

$$\phi_1(x,t) = -2\pi\langle j_1\rangle t + \frac{i}{2}\int_{-\infty}^{\infty}\frac{d\omega}{\omega}\{j_1(\omega)(e^{ik_1x} + e^{ik_2x}) + j_2(\omega)(e^{ik_1x} - e^{ik_2x})\}e^{-i\omega t}, \tag{A5}$$

where we set $k_j(-\omega) = -k_j(\omega)$. In addition, we have omitted the contribution of the zero mode π_1 because we need local correlators, and replaced the zero mode $\varphi_1(t)$ by its expectation value.

APPENDIX B: EVALUATION OF THE MEASURED HEAT FLUX

The experimentally found heat flux, defined in Eq. (40), may be written in time representation as

$$I_{\rm m} = -i\,\partial_t\left[K(t) - \frac{e^{i\langle\Delta\mu\rangle t}}{2\pi i t}\right]_{t=0}. \tag{B1}$$

Since the Hamiltonian of tunneling at QPC is local, we may use Eq. (11b) and results of Appendix A in order to evaluate the correlation function $K(t)$. The difficulty of finding this function is related to the fact that, according to Eq. (A5), the correlators of the operator $\phi_1(t)$ are determined by the currents $j_\alpha(t)$, which are in general non-Gaussian. However, in the present case, we need to take the limit $t \to 0$ in Eq. (B1). The high-order cumulants of currents originate from a nonequilibrium process and are suppressed at short times $t\Delta\mu \ll 1$. Therefore, we are allowed to evaluate $K(t)$ in Gaussian approximation.

This may be done by expanding the right-hand side of the Eq. (11b) to second order in ϕ_1:

$$\ln K(t) = \langle[\phi_1(t) - \phi_1(0)]\phi_1(0)\rangle + 2\pi i\langle j_1\rangle t, \tag{B2}$$

where the averaging is over the fluctuations of the currents j_α. We then use Eq. (A5) and the stationary correlators of the currents

$$\langle j_\alpha(\omega_1) j_\beta(\omega_2)\rangle = 2\pi S_\alpha(\omega_1)\delta_{\alpha\beta}\delta(\omega_1 + \omega_2) \tag{B3}$$

to present the electron correlation function in the following form:

$$\ln K = \ln K_{\rm n} + 2\pi i\langle j_1\rangle t - \ln t. \tag{B4}$$

Here, the fluctuation contribution reads as

$$\ln K_{\rm n} = \pi\int_{-\infty}^{\infty}\frac{d\omega}{\omega^2}(e^{-i\omega t} - 1)\{\mathbb{S}_1(\omega)[1 + \cos(\Delta k L)] + \mathbb{S}_2(\omega)[1 - \cos(\Delta k L)]\}, \tag{B5}$$

where we have introduced the excess noise spectral densities $\mathbb{S}_\alpha(\omega) = S_\alpha(\omega) - \omega\theta(\omega)/2\pi$ and $\Delta k = k_1(\omega) - k_2(\omega)$.

It is easy to see that for a nonvanishing contribution to $I_{\rm m}$, given by the expression (B1), we need to expand $\ln K_{\rm n}$ to second order in t. Note, however, that the linear in t term in this expansion adds to the corresponding term in Eq. (B4) to give $2\pi i\langle\Delta\mu\rangle t$. This follows directly from the definition (39) of the "average" bias, which in time representation may be written as $\langle\Delta\mu\rangle = 2\pi\,\partial_t[tK(t)]_{t=0}$. Therefore, only the t^2 term in $\ln K_{\rm n}$ contributes to $I_{\rm m}$, and we obtain

$$I_{\rm m} = -\frac{1}{4\pi}\partial_t^2 \ln K_{\rm n}(t)|_{t=0}. \tag{B6}$$

Finally, we use Eq. (B5) and obtain the result (48).

Next, we wish to rewrite the measured flux $I_{\rm m}$ in terms of the plasmon distributions $n_j(k) = \langle\tilde{a}_j^\dagger(k)\tilde{a}_j(k)\rangle$, $j = 1,2$. For doing so, we now use Eqs. (A1) and (A3), repeat the steps that lead to (B5), and take the limit of $L \gg L_{\rm ex}$. The result may be presented in the form

$$\ln K_{\rm n} = -\sum_j\int_0^\infty\frac{dk}{k}\,n_j(k)[1 - \cos(\omega_j t)] + \frac{1}{2}\sum_j\int_0^\infty\frac{dk}{k}(e^{-i\omega_j t} - e^{-iv_j kt}), \tag{B7}$$

where the last term is the quantum contribution due to the nonlinear plasmon spectrum, and $v_j = \partial\omega_j/\partial k$ are the plasmon speeds at $k = 0$. By substituting expressions (B7) into Eq. (B6), we obtain the final results (51) and (52) for the measured heat flux.

APPENDIX C: SUPPRESSION OF HIGHER-ORDER CUMULANTS

Here, we show that a weak dispersion of plasmon modes leads to the suppression of the contribution of higher-order cumulants of current j_α to the electron correlation function at long distances L from the source of currents. We demonstrate this by using an example of a weakly dispersive spectrum of plasmons in the form $k_j = \omega/v_j + \gamma_j\omega^2{\rm sign}(\omega)$, $j = 1,2$. Since we are interested in the behavior of the electron distribution function close to the Fermi level, we need to know a long-time asymptotics of the electron correlation function $K(t)$. Therefore, the contributing currents j_α can be considered Markovian processes and fields ϕ_α can be treated as classical variables.

Let us consider the nth cumulant

$$M^{(n)}(L,t) \equiv \langle\langle[\phi_1(L,t) - \phi_1(L,0)]^n\rangle\rangle. \tag{C1}$$

According to Eq. (A5), at large distances $L \gg L_{\rm ex} = v_j/\Delta\mu$ and long times $t\Delta\mu \gg 1$, it may be written as

$$M^{(n)}(L,t) = \sum_\alpha M_\alpha^{(n)}(L,t), \tag{C2}$$

where

$$M_\alpha^{(n)}(L,t) = 2\pi S_\alpha^{(n)} \int \prod_{l=1}^{n} \frac{d\omega_l}{\omega_l}(i/2)(e^{-i\omega_l t} - 1) \times \delta(\omega_1 + \cdots + \omega_n)\left[e^{i\sum_l k_1(\omega_l)L} + e^{i\sum_l k_2(\omega_l)L}\right] \tag{C3}$$

and $S_\alpha^{(n)} \equiv \langle\langle j_\alpha^n \rangle\rangle$. Here, we have neglected the cross terms containing fast oscillating functions. These terms have the same origin as fast oscillating terms in (48) and vanish at distances $L \gg L_{\rm ex}$. Dropping those terms is also equivalent to neglecting in (20) correlations of charges taken at different times t_u and t_v. Finally, we note that in our particular case, where the QPC is connected to the outmost edge channel only, $S_2^{(n)} = 0$ for $n > 2$.

One can easily see that $\sum_l k_j(\omega_l) = \sum_l \gamma_j \omega_l^2 \mathrm{sign}(\omega_l)$ because the integrals in (C3) are limited to $\sum_l \omega_l = 0$. For the second cumulant, this implies that $k_j(\omega_1) + k_j(\omega_2) = 0$, i.e., the dispersion correction cancels too. Therefore, the second cumulant is not suppressed at long distances. In the following, we consider high-order cumulants. Using the identity $2\pi\delta(\omega_1 + \cdots + \omega_n) = \int d\tau \exp[i(\omega_1 + \cdots + \omega_n)\tau]$, we can write

$$M_\alpha^{(n)}(L,t) = S_\alpha^{(n)} \sum_j \int_{-\infty}^{\infty} d\tau [F_j(\tau,t,L)]^n, \tag{C4}$$

where we have introduced the integrals

$$F_j = \frac{i}{2}\int \frac{d\omega}{\omega}(e^{-i\omega t} - 1)e^{i\omega\tau + i\gamma_j L\omega^2 \mathrm{sign}(\omega)}. \tag{C5}$$

At large distances $L\gamma_j \gg t^2$, the contribution to the integrals F_j comes from small ω, where one can approximate $e^{-i\omega t} - 1 \approx -i\omega t$. Therefore, Eq. (C5) can be further simplified:

$$F_j = (t/2)\int d\omega\, e^{i\omega\tau + i\gamma_j L\omega^2 \mathrm{sign}(\omega)} \propto \frac{t}{\sqrt{\gamma_j L}} e^{\pm i\tau^2/4\gamma_j L}. \tag{C6}$$

By substituting this result into Eq. (C4) and then to (C2), we find that

$$M^{(n)}(L,t) \propto t \sum_\alpha S_\alpha^{(n)} \sum_{j=1,2} \left(\frac{t^2}{\gamma_j L}\right)^{\frac{n-1}{2}}, \quad n > 2 \tag{C7}$$

where, we recall, the sum is over the plasmon eigenmode number j and over the channel number α.

We note that, at large distances L, the cumulants $M^{(n)}(L,t)$ are suppressed by the dimensionless small parameter $t^2/\gamma_j L \ll 1$. Therefore, the distribution function at the energy ϵ is determined by the Gaussian part of the noise, if $L \gg 1/\gamma_j \epsilon^2$. In our case, $S_1^{(n)} \sim T\Delta\mu$ and $S_2^{(n)} = 0$, and the contribution of high-order cumulants to the correlator $K(t)$ may be neglected at distances larger than $L_{\rm g} = 1/\gamma_j (T\Delta\mu)^2$, so that the noise may be considered Gaussian. Obviously, if only one plasmon mode of two is dispersive, e.g., $\gamma_2 = 0$, then at distances $L \gg L_{\rm g}$, the cumulant (C2) is suppressed by the factor of 2. One can interpret the result (C7) as the renormalization of the effective coupling constant λ in (13), which is caused by spreading of plasmon wave packets due to the dispersion.

[1] K. V. Klitzing, G. Dorda, and M. Pepper, Phys. Rev. Lett. **45**, 494 (1980).

[2] Y. Ji, Y. Chung, D. Sprinzak, M. Heiblum, D. Mahalu, and H. Shtrikman, Nature (London) **422**, 415 (2003).

[3] I. Neder, M. Heiblum, Y. Levinson, D. Mahalu, and V. Umansky, Phys. Rev. Lett. **96**, 016804 (2006); I. Neder, F. Marquardt, M. Heiblum, D. Mahalu, and V. Umansky, Nat. Phys. **3**, 534 (2007).

[4] P. Roulleau, F. Portier, D. C. Glattli, P. Roche, A. Cavanna, G. Faini, U. Gennser, and D. Mailly, Phys. Rev. B **76**, 161309(R) (2007); Phys. Rev. Lett. **100**, 126802 (2008).

[5] L. V. Litvin, H.-P. Tranitz, W. Wegscheider, and C. Strunk, Phys. Rev. B **75**, 033315 (2007); L. V. Litvin, A. Helzel, H.-P. Tranitz, W. Wegscheider, and C. Strunk, *ibid.* **78**, 075303 (2008).

[6] E. Bieri, M. Weiss, O. Goktas, M. Hauser, C. Schonenberger, and S. Oberholzer, Phys. Rev. B **79**, 245324 (2009).

[7] B. I. Halperin, Phys. Rev. B **25**, 2185 (1982); M. Büttiker, *ibid.* **38**, 9375 (1988) and references therein.

[8] V. A. Volkov and S. A. Mikhailov, Zh. Eksp. Teor. Fiz. **94**, 217 (1988) [Sov. Phys.–JETP **67**, 1639 (1988)]; D. B. Chklovskii, B. I. Shklovskii, and L. I. Glazman, Phys. Rev. B **46**, 4026 (1992); I. L. Aleiner and L. I. Glazman, Phys. Rev. Lett. **72**, 2935 (1994); C. de C. Chamon and X. G. Wen, Phys. Rev. B **49**, 8227 (1994), and references therein.

[9] X.-G. Wen, Phys. Rev. B **41**, 12838 (1990); J. Fröhlich and A. Zee, Nucl. Phys. B **364**, 517 (1991).

[10] For a review, see A. M. Chang, Rev. Mod. Phys. **75**, 1449 (2003).

[11] E. V. Sukhorukov and V. V. Cheianov, Phys. Rev. Lett. **99**, 156801 (2007).

[12] J. T. Chalker, Y. Gefen, and M. Y. Veillette, Phys. Rev. B **76**, 085320 (2007).

[13] I. P. Levkivskyi and E. V. Sukhorukov, Phys. Rev. B **78**, 045322 (2008).

[14] I. Neder and E. Ginossar, Phys. Rev. Lett. **100**, 196806 (2008).

[15] S.-C. Youn, H.-W. Lee, and H.-S. Sim, Phys. Rev. Lett. **100**, 196807 (2008).

[16] C. L. Kane and M. P. A. Fisher, Phys. Rev. B **52**, 17393 (1995); V. V. Ponomarenko and D. V. Averin, *ibid.* **67**, 035314 (2003); D. B. Gutman, Y. Gefen, and A. D. Mirlin, Eur. Phys. Lett. **90**, 37003 (2010); D. L. Kovrizhin and J. T. Chalker, Phys. Rev. B **84**, 085105 (2011).

[17] L. P. Kouwenhoven, B. J. van Wees, N. C. van der Vaart, C. J. P. M. Harmans, C. E. Timmering, and C. T. Foxon, Phys. Rev. Lett. **64**, 685 (1990); H. Pothier, S. Guéron, N. O. Birge, D. Esteve, and M. H. Devoret, *ibid.* **79**, 3490 (1997); A. Anthore, F. Pierre, H. Pothier, and D. Esteve, *ibid.* **90**, 076806 (2003); G. Granger, J. P. Eisenstein, and J. L. Reno, *ibid.* **102**, 086803 (2009).

[18]C. Altimiras, H. le Sueur, U. Gennser, A. Cavanna, D. Mailly, and F. Pierre, Nat. Phys. **6**, 34 (2010).

[19]H. le Sueur, C. Altimiras, U. Gennser, A. Cavanna, D. Mailly, and F. Pierre, Phys. Rev. Lett. **105**, 056803 (2010); C. Altimiras, H. le Sueur, U. Gennser, A. Cavanna, D. Mailly, and F. Pierre, *ibid.* **105**, 226804 (2010).

[20]A. M. Lunde, S. E. Nigg, and M. Buttiker, Phys. Rev. B **81**, 041311(R) (2010).

[21]P. Degiovanni, Ch. Grenier, G. Fève, C. Altimiras, H. le Sueur, and F. Pierre, Phys. Rev. B **81**, 121302(R) (2010).

[22]In fact, exactly the same physical effect leads to the decoherence in MZ interferometers (Refs. 3–6) and is responsible for the anomalous dephasing, as demonstrated in our earlier work (Ref. 23).

[23]I. P. Levkivskyi and E. V. Sukhorukov, Phys. Rev. Lett. **103**, 036801 (2009).

[24]L. S. Levitov, H. Lee, and G. B. Lesovik, J. Math. Phys. **37**, 4845 (1996).

[25]Th. Giamarchi, *Quantum Physics in One Dimension* (Oxford University Press, Oxford, 2003).

[26]Note that the problem of finding the conductance of a 1D system attached to Ohmic reservoirs requires a different type of boundary conditions for fields ϕ_α, imposed at reservoirs, where currents are classical variables. See, e.g., I. Safi, Eur. Phys. J. B. **12**, 451 (1999).

[27]For a recent experiment, see C. Altimiras, U. Gennser, A. Cavanna, D. Mailly, and F. Pierre, Phys. Rev. Lett. **99**, 256805 (2007).

[28]K. E. Nagaev, Phys. Rev. B **66**, 075334 (2002).

[29]We would like to reiterate the role of the interaction at filling factor $\nu = 2$ by comparing to the situation at $\nu = 1$. In the last case, there is only one channel at the edge, so that the solution of the equation of motion acquires the form $\phi(x,t) = 2\pi\, Q(t - x/u)$, and the correlation function (20) is given by $\chi(2\pi,t)$. One can show that this correlation function describes free electrons, therefore, the screened Coulomb interaction leads solely to the renormalization of the Fermi velocity.

[30]E. V. Sukhorukov and J. Edwards, Phys. Rev. B **78**, 035332 (2008).

[31]H. B. Callen and T. A. Welton, Phys. Rev. **83**, 34 (1951).

[32]For a review, see Y. M. Blanter and M. Büttiker, Phys. Rep. **336**, 1 (1986).

[33]We choose this example of the dispersion correction in the spectrum merely to do estimates, and to draw general conclusions, and not as a realistic example.

[34]We note that in general the heat flux can not be associated with a conserved Noether current because the Hamiltonian (6) is not local. Nevertheless, the continuity equation for the heat flux I_h, given by (55), may be derived in the semiclassical limit $kv < \Delta\mu$, which is of interest here. Moreover, one can show that for any interaction matrix (9), the energy flux of zero modes of plasmons does not contribute to the total heat flux if it is defined as the Joule heat created at the QPC.